Amphoteric and Controllable Doping of Carbon Nanotubes by Encapsulation of Organic and Organometallic Molecules

Jing Lu,[1,2,*] Shigeru Nagase,[1,†] Dapeng Yu,[2] Hengqiang Ye,[2] Rushan Han,[2] Zhengxiang Gao,[2] Shuang Zhang,[3] and Lianmao Peng[3]

[1]*Department of Theoretical Studies, Institute for Molecular Science, Okazaki 444-8585, Japan*
[2]*Mesoscopic Physics Laboratory, Department of Physics, Peking University, Beijing 100871, People's Republic of China*
[3]*Department of Electronics, Peking University, Beijing 100871, People's Republic of China*

(Received 10 February 2004; published 10 September 2004)

By using first principles calculations, we show that fine tuning of both *p*- and *n*-type doping can be realized on single-wall carbon nanotubes (SWNTs) by tuning the electron affinity or ionization potential of the organic and organometallic molecules encapsulated inside SWNTs. This novel type of SWNT-based material offers great promise for molecular electronics because of its air stability, synthetic simplicity and the abundance of organic and organometallic molecules.

DOI: 10.1103/PhysRevLett.93.116804 PACS numbers: 73.22.–f, 61.48.+c, 71.20.Tx

Single-wall carbon nanotubes (SWNTs) have strong potential for molecular electronics. For practical application it is crucial to obtain both *p*- and *n*-type air-stable SWNTs and control their carrier density. SWNT field-effect transistors (FETs) under ambient conditions are always *p* type due to electron withdrawing by the absorbed O_2. The production of air-stable *n*-type SWNT transistors is thus especially important technologically. Several doping methods, including adsorption of alkali metals [1], annealing in vacuum [2], inert gas [3], or hydrogen [4], and electrochemical method [5], have been developed for producing *n*-type SWNTs, but their stability in air was not satisfactory. Polymer functionalization of SWNT can yield air-stable *n*-type SWNTs with low carrier concentration [6]; however, a fine tuning of carrier concentration remains very difficult in this scheme. Very recently, air-stable amphoteric doping on SWNTs has been realized by encapsulating organic molecules inside SWNTs [7]. The characteristic optical absorption intensities of these doped SWNTs change with the electron affinity (EA) or ionization potential (IP) of the encapsulated organic molecules [7]. This suggests that the carrier concentration of SWNTs can be controlled by tuning the EA or IP of the encapsulated organic molecules. Furthermore, the process of doping SWNTs by organic molecule is simple; thus a viable route for the large-scale production of SWNTs with controllable doping state is offered.

In this Letter, we have investigated the effects of organic molecule doping on the geometrical and electronic properties of SWNTs by using density functional theory. We confirm that encapsulation of electrophilic organic molecules inside SWNTs indeed realizes a controllable *p*-type doping. Conversely, encapsulation of nucleophilic organic molecules inside SWNTs leads to a controllable *n*-type doping. Moreover, we propose a new route to create air-stable SWNTs with *n*-type doping: encapsulation of nucleophilic organometallic molecules inside SWNTs.

We choose (16,0) SWNT (diameter $d = 12.53$ Å) as representative of semiconducting SWNTs. Tetracyano-*p*-quinodimethane (TCNQ) and tetrafluorocyano-*p*-quinodimethane (F_4TCNQ) are chosen as representatives of electrophilic organic molecules with adiabatic EA (AEA) of 2.80 and 3.38 eV, respectively, while tetrathiafulvalene (TTF) and tetrakis(dimethylamino)ethylene (TDAE) are chosen as representatives of nucleophilic organic molecules with adiabatic IP (AIP) of 6.40 and 5.36 eV, respectively. The (16,0) SWNT doped by organic molecules is modeled by a periodical supercell where the periodicity of the (16,0) SWNT is commeasurable with those of organic molecules. This is, of course, a model assumption, since a supercell geometry cannot describe a truly incommensurate system. The experimentally estimated saturation intercalation density of TCNQ inside SWNTs is TCNQ/C_{140}, and those of F_4TCNQ, TTF, and TDAE are 100–150 C atoms per molecule [7]. In our supercell model the periodicity of the organic molecules is assumed to be twice that of the (16,0) SWNT and each unit cell contains 128 C atoms. We label this model by molecule@$(16, 0)$ (C_{128} unit cell). The SWNT is placed with its wall separated from another wall of an adjacent nanotube by no less than 6.0 Å.

The absence of any extra X-ray powder diffraction peaks suggested a random orientation of the encapsulated organic molecules inside SWNTs [7]. For simplicity, the C═C double bond of TDAE in our model is arranged along the tube axis, while the initial molecular long axes of TCNQ, F_4TCNQ, and TTF make an angle of 30° with the tube axis to maintain a proper distance between molecules. We have located the optimal position of the encapsulated organic molecules by calculating the dependence of the static total energy of the doped system on the distance (r) between the center of mass of the organic molecules and the tube axis. In these calculations, we used the ultrasoft pseudopotential [8] plane-wave program, CASTEP [9], with two k points. The cutoff energy for the

plane-wave basis set was 240 eV. The generalized gradient approximation by Perdew, Burke, and Ernzerhof (PBE) [10] was employed for the exchange-correlation functional. Full geometry optimization has been performed for the organic molecules and (16,0) SWNT separately prior to the static total calculation of the doped system. The TDAE molecule has C_2 symmetry from the structural determination for solid TDAE-C_{60} [11]. The optimized C=C double bond length and the torsion angle between 2 N-C-N planes are 1.362 Å and 28.53°, respectively, well comparable to the experimental ones of 1.36 Å and 28° [12]. The total energies of the doped systems as a function of r are displayed in Fig. 1. Three organic molecules: TCNQ, F_4TCNQ, and TDAE favor occupying the center of nanotube, while the TTF molecule prefers a distance of 1 Å away from the tube axis. This difference can be ascribed to the smaller projected size along the tube axis for the TTF molecule compared with the other three molecules, which allows a larger degree of freedom of TTF inside the (16,0) SWNT. Full geometry optimization was performed for both the atomic positions and lattice lengths from above starting points. The intercalation energy of an organic molecule in SWNT is defined as

$$\mathrm{IE} = E(\text{doped SWNT}) - E(\text{SWNT}) - E(\text{organic molecule})$$

A larger 312 eV plane-wave cutoff energy is used in IE calculations.

The optimized geometries of molecule@(16, 0) (C_{128} unit cell) are shown in Figs. 2(a)–2(d). The nanotube wall is almost unchanged upon encapsulation of the centrally located TCNQ, F_4TCNQ, and TDAE molecules, but it is distorted by encapsulation of the off-center TTF molecule. The degree of ellipsoidal deformation from the circular tube cross section is $r_{\max}/r_{\min} = 7\%$. The optimized oblique angles of the molecular planes of TCNQ, F_4TCNQ, and TTF relative to the tube axis are 27–28°. The closest contacts between the TCNQ, F_4TCNQ, TTF, and TDAE molecules and nanotube wall are 3.62, 3.62, 3.44, and 3.28 Å, respectively.

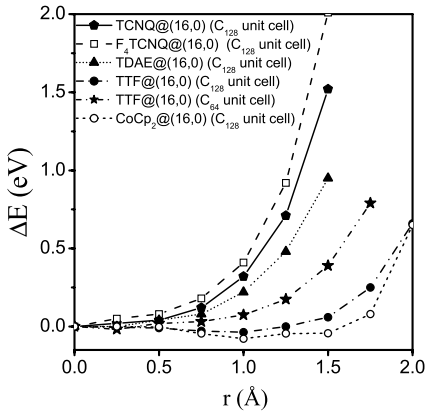

FIG. 1. Total energies ΔE of organic- and organometallic molecule doped (16,0) SWNTs as a function of the off-axis displacement r, with $\Delta E(r = 0)$ used as a reference.

The electronic band structures of molecule@(16, 0) (C_{128} unit cell) are shown in Figs. 3(a)–3(d). The flat bands near the Fermi level (E_f) labeled α are derived from the lowest unoccupied molecular orbital states of TCNQ and F_4TCNQ, and those labeled β derived from the highest occupied molecular orbital (HOMO) states of TTF and TDAE. The α bands are partially filled in TCNQ@(16, 0) (C_{128} unit cell) and F_4TCNQ@(16, 0) (C_{128} unit cell), indicative of electron transfer from the nanotube to TCNQ and F_4TCNQ. The lower-lying α band is more populated in F_4TCNQ@(16, 0) (C_{128} unit cell) than in TCNQ@(16, 0) (C_{128} unit cell). A Mulliken population analysis also confirms that the electron transfer from the (16,0) nanotube to the organic molecules increases with increasing EA of the entrapped organic molecule, and 0.32 and 0.60 electrons are transferred from the (16,0) nanotube to TCNQ and F_4TCNQ, respectively (Table I). This tendency is in agreement with the observed larger reduction in the characteristic optical absorption intensity for F_4TCNQ doped SWNT than for TCNQ doped SWNT. The β band in TTF@(16, 0) (C_{128} unit cell) lies in the middle of the gap between the nanotube conduction and valence bands, marking no appreciable electron transfer between TTF and the nanotube. The higher-lying β band in TDAE@(16, 0) (C_{128} unit cell), however, overlaps with the bottom of the nanotube conduction band, and about 0.2 electrons are transferred from TDAE to the nanotube. This difference in the band structure is apparently ascribed to the smaller IP of TDAE compared with TTF.

The TCNQ, F_4TCNQ, and TTF molecules are physisorbed inside nanotube from the calculated IEs of −0.17, −0.37, and −0.15 eV per molecule, respectively

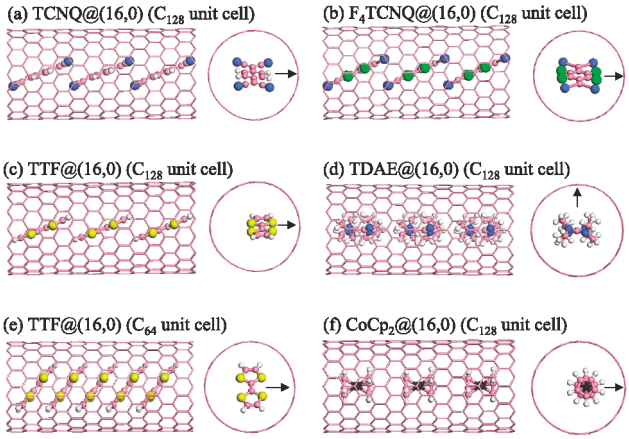

FIG. 2 (color). Geometric structures of organic- and organometallic molecule doped (16,0) SWNTs. Pink ball: C; white ball: H; blue ball: N; green ball: F; yellow ball: S; black ball: cobalt. The arrows represent the shift directions of the organic- and organometallic molecules that are used to determine the ΔE-r relation of Fig. 1.

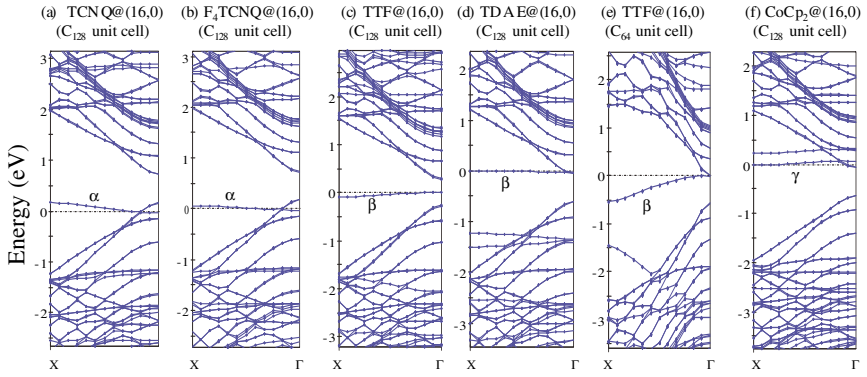

FIG. 3 (color online). Electronic band structure of the (16,0) SWNT doped by organic- and organometallic molecules, with $E_f = 0$. Bigger α-, β, and γ bandwidths than shown in this figure are expected if the random orientations of the organic- and organometallic molecules are taken into account.

(Table I). Under ambient conditions the escaping process appears unlikely once the three molecules are trapped inside the SWNT. In contrast, the encapsulation of TDAE inside the (16,0) nanotube is almost thermoneutral with IE = 0.01 eV. The encapsulated TADE is likely to escape the nanotube under ambient conditions since the escaping process costs no energy. Note that encapsulation of the organic molecules inside SWNTs is the possible cause of air stability of these doped systems as the outer nanotube wall prevents the molecules from attack by oxygen. The higher stability of TCNQ, F_4TCNQ, and TTF inside SWNTs probably accounts for the observed air stability of TCNQ-, F_4TCNQ-, and TTF doped SWNTs, whereas the easy escape of the entrapped TDAE from the nanotube appears to be responsible for the observed air instability of TDAE doped SWNTs [7].

The absence of electron transfer from TTF to the nanotube in the TTF@(16, 0) (C_{128} unit cell), however, is incompatible with the transport and optical adsorption data for TTF doped SWNTs [7]. In the charge-transfer TTF-TCNQ crystal, the closest center-to-center distance between adjacent TTF molecules along the b direction is about 3.8 Å, which gives rise to a large (~1.0 eV) dispersion for the TTF HOMO-derived band along this direction [13]. The β band (0.1 eV in dispersion) is only 0.23 eV lower than the nanotube conduction band bottom in TTF@(16, 0) (C_{128} unit cell), and an overlap between them is anticipated if the β band is sufficiently broadened due to a closer packing of the TTF molecules inside the nanotube. Alternatively, we consider a smaller supercell model for TTF doped nanotube where the periodicity of the organic molecules is identical to that of the (16,0) SWNT (labeled TTF@(16, 0) (C_{64} unit cell). In this model, the long molecular axis of TTF makes 60° angle with the tube axis. The optimized distance from the center of the TTF molecule to the tube axis is reduced to 0.25 Å to maintain the van der Waals gap between TTF and the tube wall. The deformation of the nanotube wall is significantly reduced in TTF@(16, 0) (C_{64} unit cell) [Fig. 2(e)] compared with TTF@(16, 0) (C_{128} unit cell), and the optimized angle of the long axis of TTF is 59° relative the tube axis. The β band is broadened by 0.4 eV, and overlaps with the bottom of the nanotube conduction band at the Γ point [Fig. 3(e)], accompanied by 0.12 electron transfer from TTF to the nanotube. The TTF molecules in TTF@(16, 0) (C_{64} unit cell) model are, however, overcrowded from a calculated positive IE of 0.28 eV and a comparison with the experimentally estimated saturation concentration of 100–150 C atom per TTF molecule. Therefore, in the actual saturated phase of TTF@(16, 0), the amount of electron transfer from TTF to nanotube should be smaller than $0.12e$. The smaller electron transfer of $<0.12e$ per molecule in TTF doped (16,0) SWNT compared with a value of $0.2e$ per molecule in TDAE@(16, 0) (C_{128} unit cell) is qualitatively in accord with the observed larger reduction in the characteristic optical absorption intensity for TDAE doped SWNT than for TTF doped SWNT.

From the above calculations, a fine amphoteric tuning of the SWNT carrier concentration at the low doping

TABLE I. Mulliken charge Q and intercalation energy (IE) (per molecule) of organic- and organometallic molecules inside SWNT. The measured adiabatic electron affinities (AEA's) and adiabatic ionization potentials (AIP's) are listed for the electrophilic and nucleophilic molecules, respectively.

	Unit cell size	Q (e)	AEA (eV)	AIP (eV)	IE (eV)
TCNQ@(16, 0)	C_{128}	−0.32	2.80 [7], 3.68[a]		−0.17
F_4TCNQ@(16, 0)	C_{128}	−0.60	3.38 [7], 4.09[a]		−0.37
TTF@(16, 0)	C_{128}	0		6.40 [7], 6.30[a]	−0.15
TDAE@(16, 0)	C_{128}	0.20		5.36 [7], 5.06[a]	0.01
TTF@(16, 0)	C_{64}	0.12			0.28
$CoCp_2$@(16, 0)	C_{128}	0.61		4.77[a]	−0.09

[a]Theoretical value of this work by using the PBE functional and DNP atomic orbital basis set.

levels can be realized by endohedral organic molecule doping. This result is striking in light of the rather difficult control of the carrier density at low densities in the case of alkali and halogen, both of which quickly produce highly doped states. The air instability of TDAE doped SWNT prompted us to consider other molecules to realize air-stable *n*-type doping on SWNT. The TDAE molecule serves as an electron donor in the organic ferromagnet TDAE-C_{60}, and a similar role is played by the organometallic molecule dicyclopentadienylcobalt ($CoCp_2$ or cobaltocene) in the organic ferromagnet $CoCp_2$ doped fullerene derivative [14]. The measured (calculated) vertical IP's is 5.55 [15] (5.01) and 5.95 [16] (5.58) eV for $CoCp_2$ and TDAE, respectively, and the calculated AIP's are 4.77 and 5.06 eV, respectively, by using the PBE functional and double-numerical plus polarization (DNP) atomic orbital basis set [17]. Therefore, $CoCp_2$ encapsulated inside SWNT is expected to donate more electrons than TDAE. We have constructed a CoCp@(16, 0) (C_{128} unit cell) model in which the fivefold axis of $CoCp_2$ is parallel to the tube axis. The optimal distance from the center of $CoCp_2$ to the tube axis is about 1 Å (Fig. 1), with the tube wall nearly intact [Fig. 2(f)]. The electronic structure of CoCp@(16, 0) (C_{128} unit cell) is shown in Fig. 3(f). The bottom (at the X point) of the half-filled band (labeled γ) of $CoCp_2$ is 0.1 eV higher in energy than the nanotube conduction band bottom, and about 0.61 electrons are transferred from the $CoCp_2$ molecule to the nanotube. The $CoCp_2$ molecule is slightly bound (IE $= -0.09$ eV) inside the (16,0) SWNT as the TCNQ, F_4TCNQ, and TTF molecules are, suggestive of possible air stability of $CoCp_2$@(16, 0) (C_{128} unit cell). The doping of organometallic molecule inside SWNTs is expected to be realized by a technique similar to doping SWNTs with organic molecules.

In summary, we have shown theoretically for the first time that the semiconducting SWNTs can be amphoterically doped in a controllable way by tuning the electron affinity or ionization potential of the encapsulated organic or organometallic molecule. These results agree well with the recent optical absorption and transport measurements on organic molecule doped SWNTs [7]. Along with the advantages in air stability, synthesis simplicity, and abundance of the dopant, organic- and organometallic molecule doped SWNTs are probably the first nanotube semiconductors that satisfy the requirements of practical application and promise to push the performance limit of SWNT-based devices for molecular electronics.

This work was supported by the Grant-in-Aid for NAREGI Nanoscience Project and Scientific Research on Priority Area (A) from the MEXT of Japan, and by the NSFC (Grants No. 10104001, No. 20151002, No. 90206048, and No. 90207009). We thank T. Takano for helpful discussion about their experiments of amphoteric doping of SWNTs via encapsulation of organic molecules, and Dr. S. Y. Re and K. Kobayashi for providing the initial structures of some organic molecules. We are grateful to Professor Peter Pulay for reading this manuscript carefully.

*Electronic address: jinglu@pku.edu.cn
†Electronic address: nagase@ims.ac.jp

[1] C. W. Zhou, J. Kong, E. Yenilmez, and H. J. Dai, Science **290**, 1552 (2000); S. Kazaoui, N. Minami, R. Jacquemin, H. Kataura, and Y. Achiba, Phys. Rev. B **60**, 13 339 (1999).
[2] V. Derycke, R. Martel, J. Appenzeller, and P. Avouris, Appl. Phys. Lett. **80**, 2773 (2002).
[3] R. Martel, V. Derycke, C. Lavoie, J. Appenzeller, K. K. Chan, J. Tersoff, and P. Avouris, Phys. Rev. Lett. **87**, 256805 (2001).
[4] A. Javey, H. Kim, M. Brink, Q. Wang, A. Ural, J. Guo, P. McIntyre, P. McEuen, M. Lundstrom, and H. J. Dai, Nat. Mater. **1**, 241 (2002).
[5] S. Kazaoui, N. Minami, N. Matsuda, H. Kataura, and Y. Achiba, Appl. Phys. Lett. **78**, 3433 (2001).
[6] M. Shim, A. Javey, N. W. S. Kam, and H. J. Dai, J. Am. Chem. Soc. **123**, 11512 (2001).
[7] T. Takenobu, T. Takano, M. Shiraishi, Y. Murakami, M. Ata, H. Kataura, Y. Achiba, and Y. Iwasa, Nat. Mater. **2**, 683 (2003).
[8] D. Vanderbilt, Phys. Rev. B **41**, 7892 (1990).
[9] V. Milman, B. Winkler, J. A. White, C. J. Pickard, M. C. Payne, E. V. Akhmatskaya, and R. H. Nobes, Int. J. Quantum Chem. **77**, 895 (2000).
[10] J. P. Perdew, K. Burke, and M. Ernzerhof, Phys. Rev. Lett. **77**, 3865 (1996).
[11] P. W. Stephens, D. Cox, J. W. Lauher, L. Mihaly, J. B. Wiley, P. M. Allemand, A. Hirsch, K. Holczer, Q. Li, J. D. Thompson, and F. Wudl, Nature (London) **355**, 331 (1992).
[12] H. Bock, H. Borrmann, Z. Havlas, H. Oberhammer, K. Ruppert, and A. Simon, Angew Chem. Int. Ed. Eng. **30**, 1678 (1991).
[13] S. Ishibashi and M. Kohyama, Phys. Rev. B **62**, 7839 (2000).
[14] A. Mrzel, A. Omerzu, P. Umek, D. Mihailovic, Z. Jaglicic, and Z. Trontelj, Chem. Phys. Lett. **298**, 329 (1998).
[15] C. Cauletti, J. C. Green, M. R. Kelly, P. Powell, and J. Van Tilborg, J. Electron Spectrosc. Relat. Phenom. **19**, 327 (1980).
[16] B. Cetinkaya, G. H. King, S. S. Kirshnamurthy, M. F. Lappert, and J. B. Pedley, J. Chem. Soc. D Chem. Commun. No. 21, 1370 (1971).
[17] B. Delley, J. Chem. Phys. **113**, 7756 (2000).